Universal gut microbial relationships in the gut microbiome of wild baboons

Authors: Kimberly E. Roche[1], Johannes R. Björk[2,3,4], Mauna R. Dasari[4,5], Laura Grieneisen[6,7], David Jansen[4], Trevor J. Gould[6], Laurence R. Gesquiere[8], Luis B. Barreiro[9,10,11], Susan C. Alberts[8,12,13], Ran Blekhman[6,14], Jack A. Gilbert[15], Jenny Tung[8,12,13,16], Sayan Mukherjee[1,17,18,19], Elizabeth A. Archie[4]

Affiliations:

[1] Program in Computational Biology and Bioinformatics, Duke University, Durham, NC, USA

[2] University of Groningen and University Medical Center Groningen, Department of Gastroenterology and Hepatology, Groningen, The Netherlands

[3] University of Groningen and University Medical Center Groningen, Department of Genetics, Groningen, The Netherlands

[4] Department of Biological Sciences, University of Notre Dame, Notre Dame, IN, USA

[5] Department of Biological Sciences, University of Pittsburgh, Pittsburgh, PA, USA

[6] Department of Genetics, Cell Biology, and Development, University of Minnesota, Minneapolis, MN, USA

[7] Department of Biology, University of British Columbia-Okanagan Campus, Kelowna, BC, Canada

[8] Department of Biology, Duke University, Durham, NC, USA

[9] Committee on Genetics, Genomics, and Systems Biology, University of Chicago, Chicago, IL, USA.

[10] Section of Genetic Medicine, Department of Medicine, University of Chicago, Chicago, IL, USA.

[11] Committee on Immunology, University of Chicago, Chicago, IL, USA.

[12] Department of Evolutionary Anthropology, Duke University, Durham, NC, USA

[13] Duke University Population Research Institute, Duke University, Durham, NC, USA

[14] Department of Ecology, Evolution, and Behavior, University of Minnesota, Minneapolis, MN, USA

[15] Department of Pediatrics and the Scripps Institution of Oceanography, University of California, San Diego, San Diego, CA, USA

[16] Department of Primate Behavior and Evolution, Max Planck Institute for Evolutionary Anthropology, 04103 Leipzig, Germany

[17] Departments of Statistical Science, Mathematics, Computer Science, and Bioinformatics & Biostatistics, Duke University, Durham, NC, USA

[18] Center for Scalable Data Analytics and Artificial Intelligence, University of Leipzig, Leipzig Germany

[19] Max Plank Institute for Mathematics in the Natural Sciences, Leipzig, Germany

* Correspondence to: earchie@nd.edu

Abstract

Ecological relationships between bacteria mediate the services that gut microbiomes provide to their hosts. Knowing the overall direction and strength of these relationships within hosts, and their generalizability across hosts, is essential to learn how microbial ecology scales up to affect microbiome assembly, dynamics, and host health. Here we gain insight into these patterns by inferring thousands of correlations in bacterial abundance between pairs of gut microbiome taxa from extensive time series data (5,534 microbiome profiles from 56 wild baboon hosts over a 13-year period). We model these time series using a statistically robust, multinomial logistic-normal modeling framework and test the degree to which bacterial abundance correlations are consistent across hosts (i.e., "universal") or individualized to each host. We also compare these patterns to two publicly available human data sets. We find that baboon gut microbial relationships are largely universal: correlation patterns within each baboon host reflect a mixture of idiosyncratic and shared patterns, but the shared pattern dominates by almost 2-fold. Surprisingly, the strongest and most consistently correlated bacterial pairs across hosts were overwhelmingly positively correlated and typically belonged to the same family—a 3-fold enrichment compared to pairs drawn from the data set as a whole. The bias towards universal, positive bacterial correlations was also apparent in monthly samples from human infants, and bacterial families that had universal relationships in baboons also tended to be universal in human infants. Together, our results advance our understanding of the relationships that shape gut microbial ecosystems, with implications for microbiome personalization, community assembly and stability, and the feasibility of microbiome interventions to improve host health.

Introduction

Mammalian gut microbiomes are highly diverse, dynamic communities whose members exhibit the full spectrum of ecological relationships, from strong mutualisms like syntrophy and cross-feeding, to competition, parasitism, and predation [1-4]. These relationships mediate a variety of biological processes that have powerful effects on host health and fitness, including the metabolism of complex carbohydrates and toxins, and the synthesis of physiologically important compounds, like short-chain fatty acids, neurotransmitters, and vitamins [1-8]. Despite their importance, major gaps remain in our understanding of microbial relationships in the gut microbiome [1, 9, 10]. We typically do not know if the abundance of one microbe consistently predicts the abundance of other microbes in the same host community, nor do we understand whether these correlative relationships are consistent in strength or direction across hosts ([10-13]).

Knowing the overall direction and strength of these correlative relationships is important, not only because they partly reflect the ecological relationships that mediate gut microbial processes, but also because overall correlation patterns can affect gut microbiome assembly, stability, and productivity [14, 15]. For instance, sets of microbes that exhibit strong, positive relationships within hosts sometimes represent networks of cooperating taxa that promote each other's growth [5, 9, 16]. In turn, these strong, mutualistic interdependencies can create an ecological house of cards where microbes rise and fall together, hampering community assembly and stability [14, 17]. In addition, understanding the degree to which correlative relationships between microbes are the same or different in different hosts can shed light on whether hosts share similar, underlying microbial ecologies [9, 10, 18-20]. Filling this knowledge gap has consequences for the generalizability of microbiome assembly processes, stability, and the

86 ecosystem services that emerge from microbiome dynamics to affect host health [9, 10, 12, 14,
87 17, 21].
88   To date, there are several reasons to think that correlative relationships in the gut
89 microbiome will not be consistent across hosts and will instead be individualized to each host.
90 For instance, several common community and evolutionary processes—such as horizontal gene
91 transfer, genotype by environment interactions, and priority effects—can lead microbiome taxa
92 to fill different ecological roles in different hosts [3, 22-26]. Further, some microbes can adopt
93 context-dependent metabolisms and ecological roles depending on their microbial neighbors or
94 other aspects of the environment—all phenomena that could lead to personalized interspecies
95 relationships in gut microbiota [27-30]. Finally, the common observation that gut microbial
96 community compositions (i.e., the presence and abundance of taxa) are highly individualized is
97 sometimes proposed to arise from host-specific microbial ecologies and relationships [22-26, 31-
98 35].
99   However, to date, the handful of studies that have tested the generalizability of gut
100 microbial relationships across hosts suggest that these relationships are not highly individualized
101 and are instead largely consistent (i.e., "universal") across hosts (**Fig. 1A**; [10, 18-20, 36]). For
102 instance, Bashan et al. [10] inferred "universal" gut microbial relationships in the human gut
103 microbiome by applying dissimilarity-overlap analysis (DOA) to cross-sectional samples from
104 several human data sets. DOA infers universal microbial relationships by testing whether pairs of
105 hosts who share many of the same microbiome taxa also tend to have similar abundances of
106 those taxa [10, 18-20, 36]. This approach relies on the assumption that, when two communities
107 share many of the same species and have similar abundances of those species, they do so because
108 of a shared, underlying set of between-species abundance relationships [10, 36]. While many
109 studies using this approach find evidence that microbial relationships are "universal" [10, 18-20],
110 DOA's assumptions have been questioned because some conditions can lead to the spurious
111 detection of universality, including environmental gradients, the strength of stochastic processes,
112 and the presence of many non-interactive species [10, 36, 37].
113   An obvious alternative is to measure microbial correlations directly from microbiome
114 time series collected from several hosts [9, 38]. Unlike DOA, this approach should be able to
115 pinpoint which microbiome taxa exhibit the most and least consistent relationships across hosts.
116 However, measuring microbial correlations from longitudinal, multi-host microbiome time series
117 has its own challenges: time series with adequately dense sampling are rare, and most such data
118 sets exhibit temporal autocorrelation and irregular sampling [38]. Further, the most common, and
119 still most feasible, way to collect microbiome community data—via high-throughput
120 sequencing—generates noisy count data that usually can only be interpreted in terms of relative
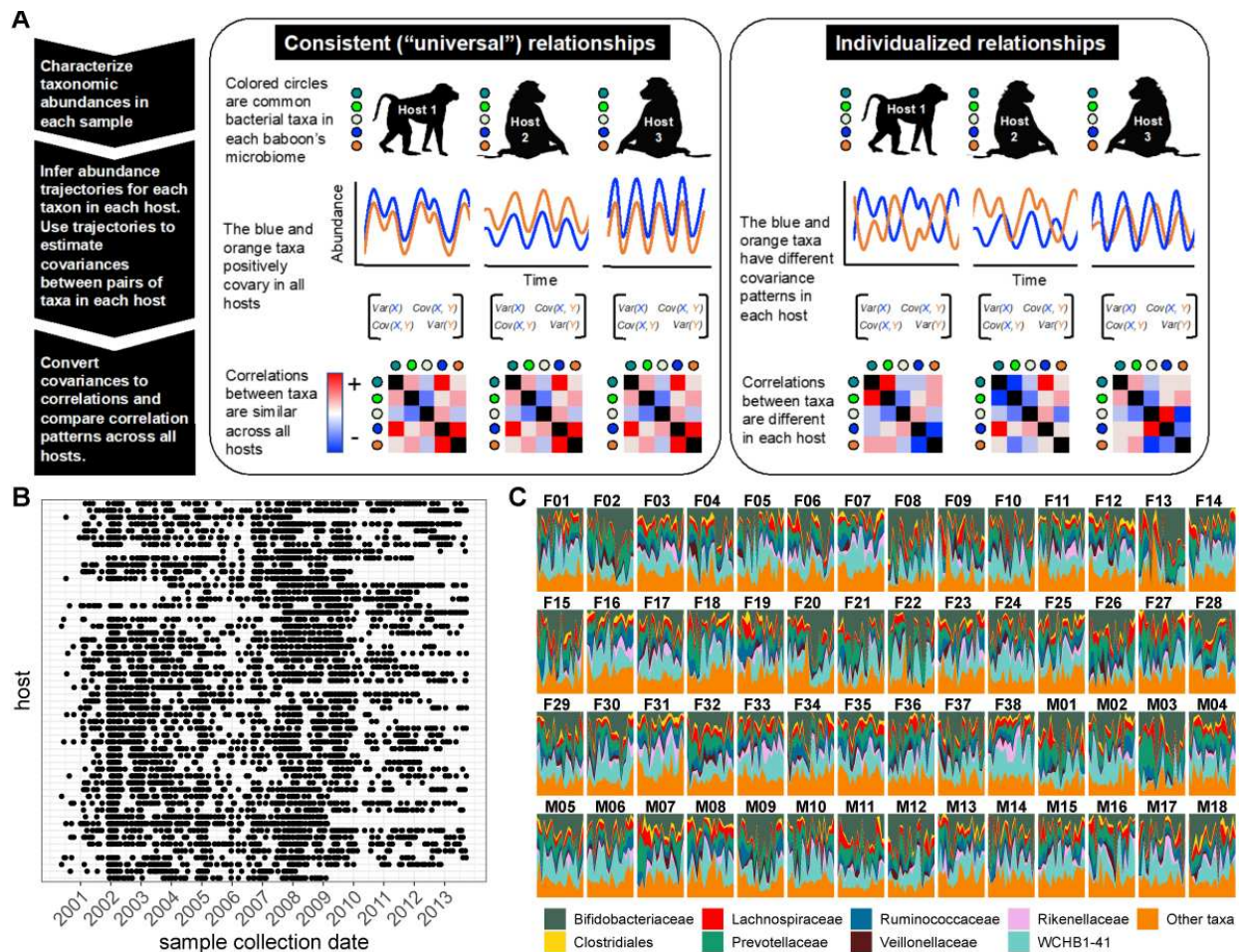121 (not absolute) abundances [39, 40].
122   To overcome these hurdles, here we combine extensive time-series data on the stool-
123 associated microbiota with a multinomial logistic-normal modeling framework (**Fig. 1;** n=5,534
124 samples from 56 baboons; 75 to 181 samples per baboon across 6 to 13.3 years, between 2000
125 and 2013; [41-43]). This framework uses 16S rRNA sequencing count data to learn a smoothly
126 evolving Gaussian process. The baboon hosts were the subject of long-term research on
127 individually recognized animals by the Amboseli Baboon Research Project in Kenya, which has
128 been studying baboon ecology and behavior in the Amboseli ecosystem since 1971 [41]. The
129 baboons range over the same habitat and experience similar diets and sources of microbial
130 colonization, facilitating inference about the consistency of microbial correlations across hosts
131 (**Fig. S1;** [42, 43]). Our modeling approach accounts for variation attributable to seasonal

132   changes in the animals' diets, proportionality in the count data, and irregularity in sampling to
133   produce per-individual, per-taxon trajectories of log-ratio abundances that we used to estimate
134   pairwise microbial correlations within each host.
135   We pursued four main objectives. First, we characterized the overall sign and strength of
136   pairwise correlations in bacterial abundance within each host. Second, we tested the degree to
137   which these correlation patterns are systematically consistent across hosts or individualized by
138   host (**Fig. 1A**). Third, we identified taxonomic, phylogenetic, environmental, and host-related
139   predictors of the direction and universality of bacterial correlations. Finally, we tested the
140   generalizability of our findings by comparing the patterns of universality in our data set to two
141   microbiome time series from humans [34, 44].
142   Our predictions for these analyses were influenced by ideas from community and
143   microbial ecology. First, because strong interdependencies can hamper community assembly and
144   destabilize community dynamics [14, 15, 17], we expected that most microbial correlations
145   would be weak with few strong positive relationships between microbes. Second, consistent with
146   studies that used DOA, we expected that microbial relationships would be more consistent across
147   hosts than individualized (see **Fig. 1A** for a visualization of this prediction). This result would
148   suggest that personalized microbiota—their compositions and dynamics—do not arise from host-
149   specific microbiome ecologies [10, 18-20]. Third, because closely related gut bacteria may have
150   similar functional properties, we expected to observe many positive correlations between those
151   that are close phylogenetic relatives. Alternatively, competitive exclusion may lead closely
152   related taxa to exhibit neutral or negative relationships. Fourth, because the environments
153   experienced by baboons in Amboseli are far more uniform than those experienced by typical
154   human study subjects [42, 43], we expected that the signature of "universality" in baboons would
155   be stronger than that observed in humans. We discuss the implications of these patterns for
156   individual microbiome community assembly and dynamics, and for understanding how
157   microbiome communities are structured across hosts—a key requirement for successful
158   intervention to improve host health [10, 11, 45].

Figure 1. Testing the generalizability of gut microbial correlations across hosts. (A)
Schematic illustrating our approach for testing the degree to which gut microbial abundance
correlations are consistent (i.e., "universal" [10]) across different baboon hosts. The left-hand set
of images show our expectations for consistent correlation patterns; the right-hand images show
our expectation for individualized correlation patterns. Colored circles next to each baboon
represent prevalent microbial taxa found in at least 20% of samples in each host (and excluding
putative duplicate 16S gene copies; see methods). In each host, we inferred centered log-ratio
(CLR) abundance trajectories for these taxa using a multinomial-logistic normal modeling
approach implemented in the R package 'fido' [46]. Cartoons of two such trajectories for the
orange and blue taxa are below each baboon. We used these trajectories to infer covariances
between each pair of taxa in all baboons (represented by covariance matrices). We then
converted these covariances to Pearson's correlations and compared bacterial correlation patterns
across all hosts, shown as heat maps (red cells are positively correlated taxa; blue cells reflect
negatively correlated taxa). **(B)** Irregular time series of fecal samples used to infer microbial
CLR abundance trajectories in 56 baboon hosts (n=5,534 total samples; 75-181 samples per
baboon across 6 to 13.3 years). Each point represents a fecal sample collected from a known
individual baboon (y-axis) on a given date (x-axis). Samples from the same baboon were
collected a median of 20 days apart (range=0 to 723 days; 25th percentile=7 days, 75th
percentile =49 days). **(C)** Relative abundances of the 8 most prevalent gut bacterial orders and

5

179   families over time (x-axis) for all 56 hosts (samples from females are labeled with an F; male
180   samples with an M). Microbiota were somewhat individualized to each host (**Fig. S2**; [42, 43]).
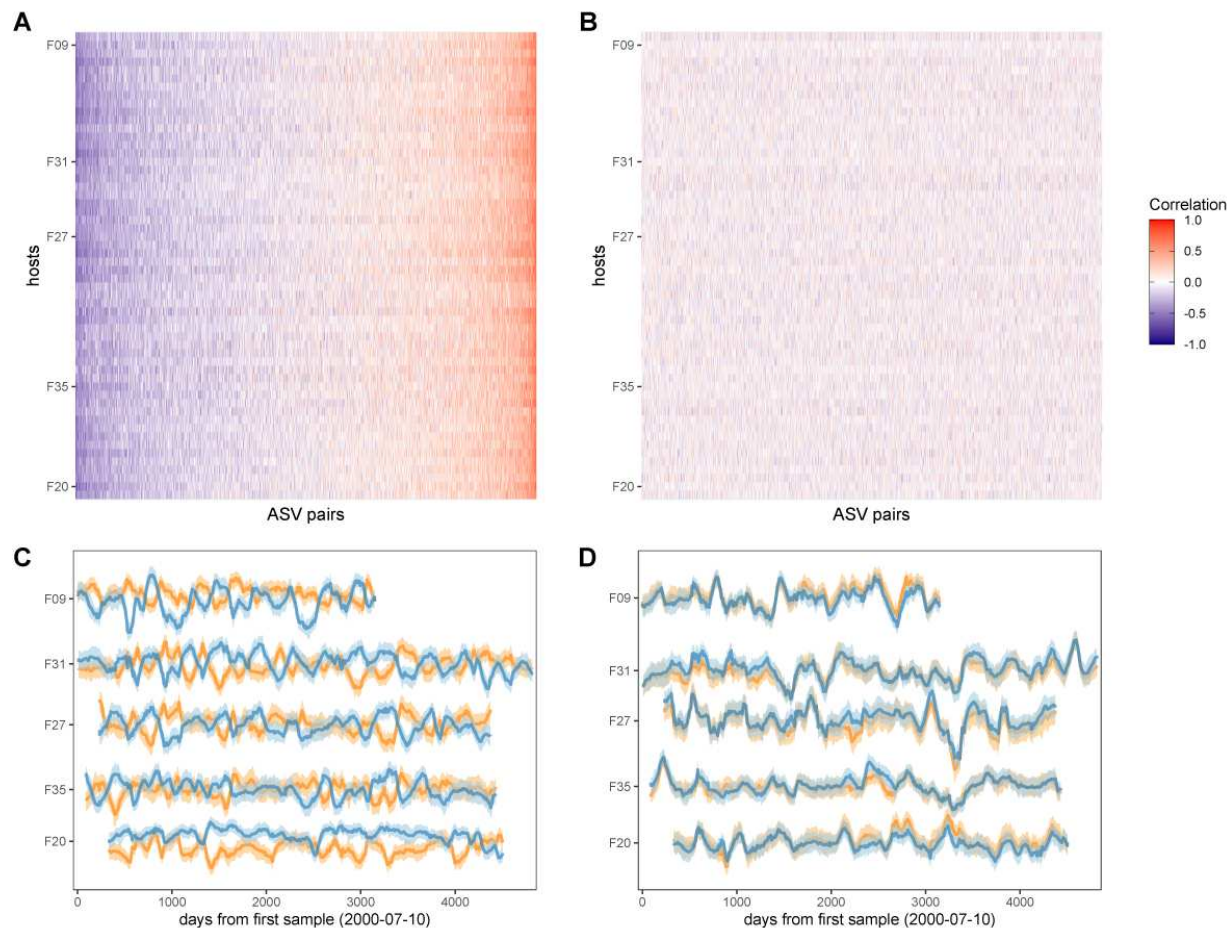181
182

Results
Most bacterial correlations within individuals are weak and negative

185   We began by characterizing the overall sign, strength, and significance of pairwise
186   correlations in bacterial abundance within each host. To do so, we applied the approach outlined
187   in **Fig. 1A** to stool-associated time series from 56 baboons (**Fig. 1B**) and calculated Pearson's
188   correlations between all possible pairs of bacterial taxa for three taxonomic partitions of the data.
189   These partitions were: (1) all pairs of CLR-transformed amplicon sequence variants (ASVs)
190   found in >20% of samples in each host and were unlikely to represent a duplicate 16S rRNA
191   gene copy ([47]; see Methods; n=125 ASVs; **Fig. 2A; Table S1**); (2) all pairs of bacterial phyla
192   found in >20% of samples in each host (n=12 phyla; **Table S2; Fig. S3**); and (3) all pairs of taxa
193   agglomerated to the most granular possible family, order, or class found in >20% of samples in
194   each host (n=37 taxa; **Table S3; Fig. S3**). We assessed the false discovery rate for each
195   correlation with a threshold for significance of FDR ≤ 0.05, by comparing the nominal p-values
196   for each observed correlation to an empirical permutation-based null, obtained by shuffling
197   taxonomic identities within microbiome samples 10 times for each host and re-calculating the
198   Pearson correlation p-values obtained from the permutations (**Fig. 2B**). We also confirmed that
199   the resulting correlation patterns were insensitive to several modeling choices and were not
200   primarily driven by seasonal shifts in microbiome composition (see results below and the
201   Supplement).
202   Consistent with the expectation that most bacterial correlations in the gut microbiome are
203   weak [14, 17], only 17% of ASV-ASV correlations in the heat map in **Fig. 2A** were stronger than
204   expected by chance (FDR ≤ 0.05; **Fig. S4A**; 20% of phylum-phylum; 21% of family/order/class
205   correlations; **Fig. S3**). The strongest negatively correlated pair in **Fig. 2A** included two ASVs in
206   the family Lachnospiraceae that had a median correlation of -0.562 (+/- 0.118 s.d.) across all
207   baboon hosts (**Fig. 2C**; ASV25 and ASV107; **Tables S1** and **S4**). The strongest positively
208   correlated pair of ASVs included two members of the genus *Prevotella* that had a median
209   correlation of 0.801 (+/- 0.053 s.d.) across all baboons (**Fig. 2D**; ASV2 and ASV3; **Tables S1**
210   and **S4**). While these two ASVs were assigned to the same genus, their V4 16S DNA sequence
211   identity was 97.6%, indicating they are probably not duplicate 16S gene copies in the same taxa
212   [47] (**Table S4**).
213   In support of the idea that positive bacterial interdependencies are rare [14, 15, 17], only
214   8.8% of ASV pairs were significantly positively correlated within hosts over time, and the
215   overall bacterial correlation patterns were slightly skewed towards negative relationships—
216   especially for relationships between bacterial phyla. For instance, at the ASV-level, the median
217   correlation coefficient in **Fig. 2A** was -0.016, and 53% of these correlations were negative
218   (binomial test p < 0.0001). For family/order/class-level taxa, 55% of all correlations in were
219   negative (**Figs. S3A** and **S4A**; median family/order/class-level correlation=-0.031; binomial test
220   p < 0.0001). Correlations between phyla exhibited the strongest negative skew, with 64% of
221   phyla-phyla correlations having a negative sign (**Figs. S3B and S4A;** median phyla-level
222   correlation=-0.092; binomial test p < 0.0001). This bias towards negative relationships may
223   reflect the fact that different phyla exhibit substantial differences in metabolism and lifestyle and
224   likely respond to distinct environmental drivers.

225

226
227
Figure 2. Bacterial correlation patterns across hosts. The heat map in panel **(A)** shows Pearson's correlation coefficients of CLR abundances between all pairs of ASVs (x-axis) in each of the 56 baboon hosts (y-axis). Each pair of ASVs is represented on the x-axis, including all pairwise combinations of 125 ASVs resulting in 7,750 ASV-ASV pairs in each host (434,000 total correlations across all 56 hosts). Columns are ordered by the mean correlation coefficient between ASV-ASV pairs, from negative (blue) to positive (red). **(B)** Pairwise correlations generated from random permutations of the data. Taxonomic identities were shuffled within samples and pairwise ASV-ASV correlations were estimated to produce a null model of ASV-ASV correlation patterns within and between hosts. Column order is the same as in Panel A. Panels **(C)** and **(D)** show example trajectories of CLR abundances for two pairs of ASVs in the same five hosts. Panel **(C)** shows a strongly negatively correlated pair (median r across all hosts=-0.562; two ASVs in family Lachnospiraceae: ASV25 (orange) and ASV107 (blue); **Tables S1 and S4**) and panel **(D)** shows one strongly positively correlated pair (median r across all hosts=0.801; two ASVs in the genus Prevotella 9; ASV2 (orange) and ASV3 (blue); **Tables S1 and S4**).
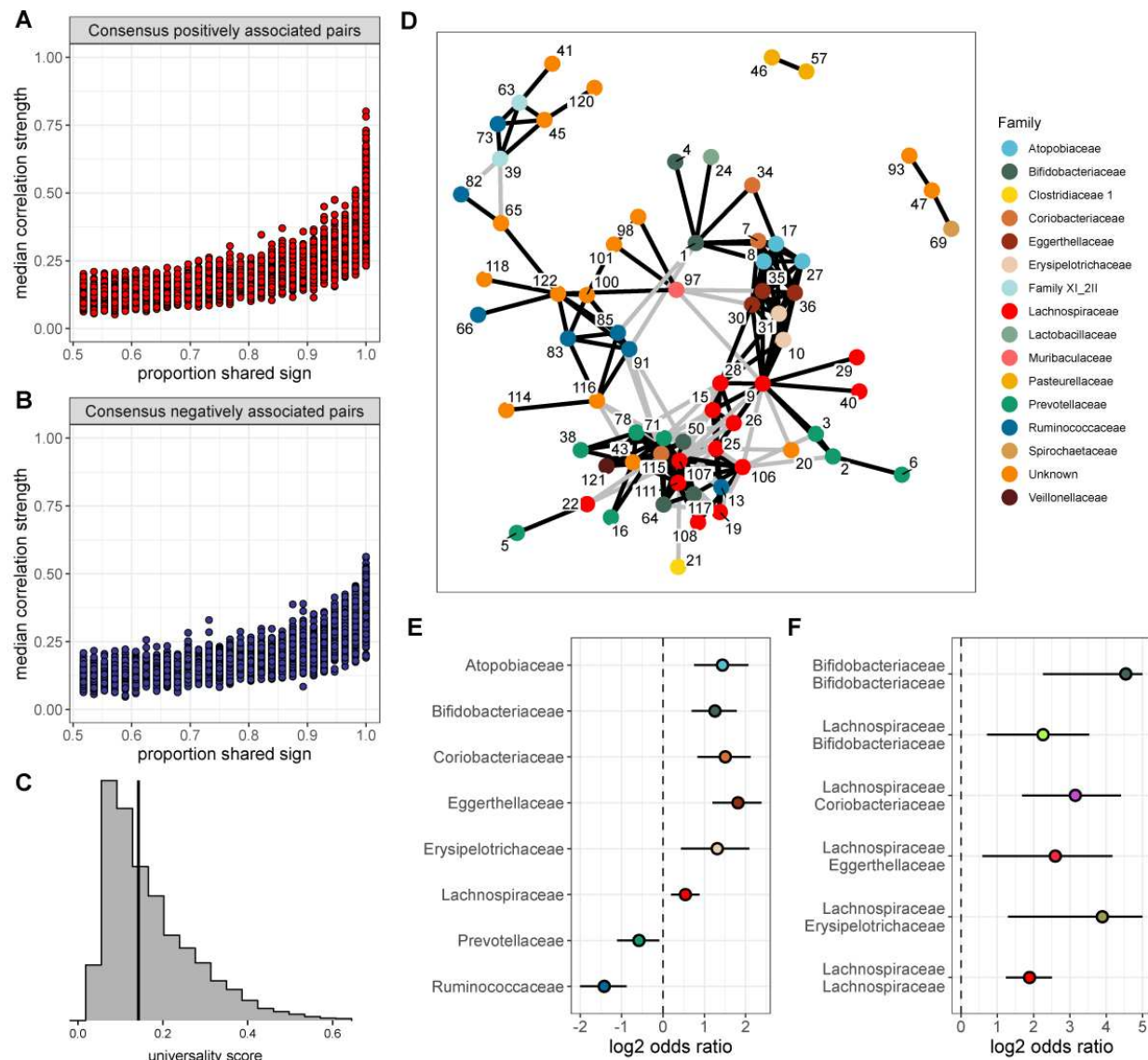
Within-host bacterial correlation patterns are largely consistent across baboons

Next, we tested the degree to which within-host ASV-ASV correlations were consistent across hosts. We began by plotting the absolute value of each ASV pair's median Pearson's correlation coefficient as a function of the consistency of their correlation sign (positive or negative) across the 56 hosts (**Figs. 3A and 3B**). These plots provide two main insights into the consistency of bacterial associations. First, in support of the idea that ASVs do not exhibit vastly different correlative relationships in different hosts, no ASV pairs were both strongly and inconsistently correlated across hosts (**Figs. 3A and 3B**; **Fig. S5A**). Instead, the ASV pairs that had inconsistent correlation signs across hosts always had weak and often non-significant median absolute correlation coefficients within hosts (**Figs. 3A and 3B**). Second, the pairs with the most consistent sign agreement across hosts also exhibited the largest median absolute correlation coefficients across hosts (**Figs. 3A and 3B**; Spearman's r=0.844, p<0.0001). Hence, pairs of ASVs that have the strongest relationships, and are therefore likely to play the most important roles in structuring gut microbiome dynamics, also tend to have the most consistent relationships in different hosts. Indeed, for the sets of positively or negatively correlated ASV-pairs that showed universal agreement in the sign of their correlation across all hosts (i.e., where x=1 in **Figs. 3A and 3B**), the median correlation coefficient is 0.398, compared to 0.113 for those with no sign consistency (x=0.5 in **Figs. 3A and 3B**). Note, that the correlation strength for a given pair of ASVs was only weakly predicted by bacterial abundance. When both members of the pair were relatively abundant, pairs tended to exhibit stronger median correlations (r=0.012, p<0.0001**; Fig. S6**). However, while this effect is significant, it explained <1% of the variance in median correlation strength.

Visual inspection of the patterns in **Figs. 2A**, **3A, and 3B** indicate that ASV-ASV correlations are largely consistent across baboons, as opposed to individualized to each baboon. To explicitly quantify the relative strength of shared versus individualized signatures in the heat map in **Fig. 2A**, we calculated the population mean pattern for the ASV-ASV correlation matrix, m. For each host, we then estimated the residual difference, e, between that individual's observed ASV-ASV correlation matrix, y, and the population mean matrix: $y - m$ (see **Fig. S7A** for a cartoon example). We reasoned that the observed correlation matrix for each host can be approximated by a mixture of contributions from the population mean matrix m and the host-specific residual matrix e. To identify the optimal mixture for each host (i.e., the mixture of consistent vs. individualized correlation patterns that best explained the observed data), we titrated the contribution (i.e., weight) of e from 0% to 100% (and correspondingly, the contribution of m from 100% to 0%) and identified the value that minimized the Frobenius distance between the simulated combination and the observed correlation matrix, y.

In support of prior observations of "universality" [10, 18-20], we found that, across hosts, the optimal mixture involved contributions from the shared correlation structure (i.e., m) of between 50% and 70% (median 65%) and a host-level contribution (i.e., from e) of between 50% and 30% (median 35%). Hence, population-level signatures contributed almost twice the weight as host-level signatures (a median population:host ratio of 1.86:1; **Fig. S7B**). As a result, ASV-level relationships tend to be more consistent across hosts than host-specific.

284
285

Figure 3. **None of the ASV pairs were strongly and inconsistently correlated across hosts, and the strongest and most consistently correlated ASVs are typically positively correlated**. Plots in (**A**) and (**B**) show the median correlation strength for each ASV-ASV pair across all 56 hosts as a function of the consistency in direction of that pair's correlation across hosts, measured as the proportion of hosts that shared the majority correlation sign (positive or negative; ASV pairs that were positively correlated in half of the 56 hosts have a consistency of 0.5; ASV pairs that were positively [or negatively] correlated in all hosts have a consistency of 1.0). Panel (**A**) presents this relationship for consensus positively correlated features and panel (**B**) shows consensus negatively correlated features. The Spearman correlation between median association strength and the proportion of shared sign for all correlated features is 0.844 (p < 0.0001). Multiplying the two axes in either panel (**A**) or (**B**) creates a "universality score", whose distribution is shown in panel (**C**). This score reflects the strength and consistency of pairwise microbial correlations across hosts and ranges from 0 to 1, where a score of 1 indicates ASV-ASV pairs with perfect correlations of the same sign in all hosts. A vertical line indicates the

9

300   minimum significant universality score. **(D)** Correlation networks for the top 2.5% most strongly
301   and consistently correlated ASV pairs across hosts (i.e., the top 2.5% highest universality scores;
302   pairs with rank 1-194 in **Table S4**). Network edges are colored by the consensus sign of the
303   correlation between that pair (black for pairs where most hosts had a positive correlation; gray
304   for pairs where most hosts had a negative correlation). Node labels indicate the ASV identity in
305   **Table S1** and colors represent bacterial families. **(E)** Significantly enriched bacterial families in
306   the network in panel D (Fisher's Exact Test p < 0.01 all, FDR ≤ 0.05; see **Table S5** enrichment
307   statistics for all families). **(F)** Significantly enriched same-family pairings in the network in panel
308   D (**Table S5**). Note that for visualization, the estimated log2 odds ratio intervals have been
309   truncated at 5; full estimates are given in **Table S5.**
310
311

The most consistent ASV-level correlations are positive and between phylogenetically related taxa
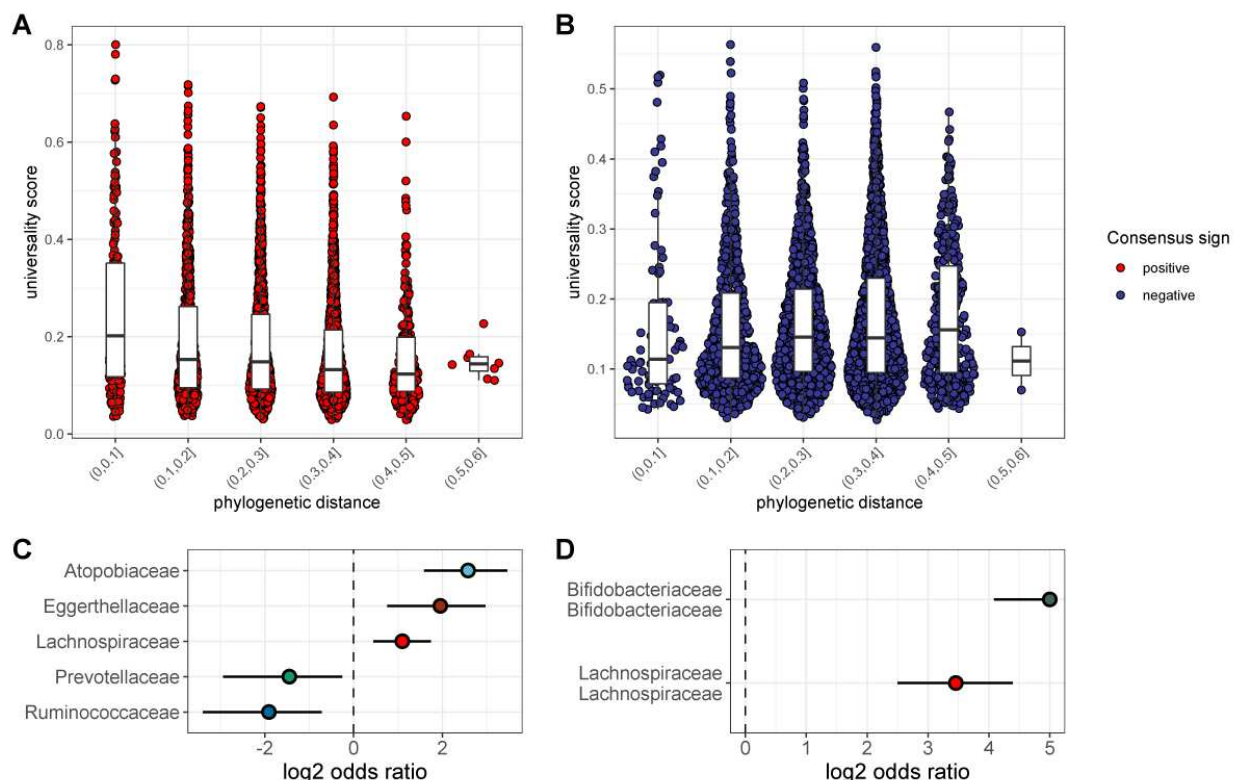
314   One advantage of our approach, compared to dissimilarity overlap analyses [10], is we
315   can identify the bacterial pairs that exhibit the most consistent relationships across hosts. Hence,
316   we next conducted several analyses to understand why some pairs of ASVs exhibit more
317   consistent correlation patterns across hosts than others. To do so, we created a "universality"
318   score that could be calculated for each ASV pair. The score multiplies the pair's median
319   correlation coefficient across hosts (y-axis of **Fig. 3A, 3B**) with its correlation consistency across
320   hosts (i.e., proportion of shared sign; x-axis of **Fig. 3A, 3B**). The resulting scores range from 0 to
321   1, where a score of 1 equates to perfect "universality" (i.e., all hosts have a correlation
322   coefficient of 1 or all hosts have a correlation coefficient of -1). Applying this score to all pairs
323   of ASVs reveals a right-skewed distribution, reflecting the fact that most bacterial correlations
324   are weak, with inconsistent sign directions across hosts (**Fig. 3C**; **Fig. S4B**). However, 49% of
325   these scores were higher than expected by chance (permutation test; FDR ≤ 0.05; **Fig. 3C**; **Fig.
326   S4B**), reflecting a signal of universality in our data.
327   Interestingly, the ASV-pairs with the highest universality scores almost always exhibited
328   net positive correlations across hosts, as opposed to net negative relationships, suggesting that
329   the most universal relationships occur between pairs of ASVs that respond similarly to shared
330   drivers or facilitate each other's growth. For example, among the ASV pairs in the top 1% of
331   universality scores (n=78 pairs), 96.2% exhibited net positive correlations across all hosts, while
332   only 5.6% (3 of 78 pairs) exhibited net negative correlations (**Table S4**). In the top 2.5% most
333   universal ASV pairs (n=194), 78.4% had net positive correlations across all hosts (**Table S4**).
334   To visualize these highly consistent positive correlations, we plotted bacterial co-
335   abundance networks connecting the top 2.5% most universal ASV pairs (**Fig. 3C**). A handful of
336   ASVs were highly connected within this network. The most connected ASV was ASV107
337   (family Lachnospiraceae; **Table S1**; **Table S4**), which was connected to 20 other ASVs. Ten
338   other ASVs were connected to more than 10 other ASVs, including six other members of
339   Lachnospiraceae (ASV9, ASV25, ASV30, ASV106, ASV107, and ASV111), two members of
340   Coriobacteria (ASV115 in the family Coriobacteriaceae and ASV30 in the genus *Slackia*), one
341   member of Bifidobacteriaceae (ASV50), and one member of Prevotellaceae (ASV71). The ASVs
342   involved in these top 2.5% pairs were enriched for the families Atopobiaceae,
343   Bifidobacteriaceae, Coriobacteriaceae, Eggerthellaceae, Erysipelotrichaceae, and
344   Lachnospiraceae (**Fig. 3E; Table S5**; all Fisher's Exact Test p-values < 0.01; FDR ≤ 0.05).

10

345   The network in **Fig. 3D** revealed clusters of positive connections, often between ASVs
346   assigned to the same family (**Fig. 3F**). In fact, same-family pairs were enriched by >3-fold in the
347   2.5% most universal taxon pairs (52 pairs observed vs. 19 expected, p < 0.0001). The cluster of
348   interconnected red nodes in **Fig. 3D** represents members of Lachnospiraceae, and
349   Lachnospiraceae-Lachnospiraceae pairings were 3.7 times more common in this network than
350   overall (30 pairs observed vs. 9 pairs expected **Fig. 3F**). Bifidobacteriaceae also tended to exhibit
351   within-family ASV pairings (**Fig. 3F**).
352   The observation that the most consistent correlations often occur among ASVs in the
353   same family raises another question: does the phylogenetic distance between a pair predict the
354   nature of their relationship? In support of the idea that closely related ASVs respond similarly to
355   the environment or facilitate each other's growth, we found a significant relationship between the
356   universality score of a given pair of ASVs and their phylogenetic distance (Pearson's r for
357   positively correlated pairs=-0.213; p < 0.0001; **Fig. 4A**). In contrast, negatively correlated ASV
358   pairs exhibited a weak positive relationship between phylogenetic distance and universality such
359   that closely related taxa tended to be less universal than more distantly related taxa (Pearson's
360   r=0.049; p=0.004; **Fig. 4B**). In other words, the strongest and most consistently *negatively*
361   correlated taxa tend to be only distantly related. Positively correlated, closely related pairs were
362   often members of the families Atopobiaceae, Eggerthellaceae, and Lachnospiraceae, especially
363   pairs where both members belonged to the family Lachnospiraceae (**Fig. 4C-D**; **Table S6).**
364

365
366   **Figure 4. The most consistent ASV-level correlations are positive and often between close**
367   **evolutionary relatives.** Pairwise universality scores are plotted as a function of phylogenetic
368   distance between the ASV-ASV pair for consensus positively correlated pairs in red (**A**) and
369   negatively correlated pairs in blue (**B**). Phylogenetic distance (x-axis) is binned into 0.1
370   increments; each point represents a given ASV pair, and box plots represent the median and
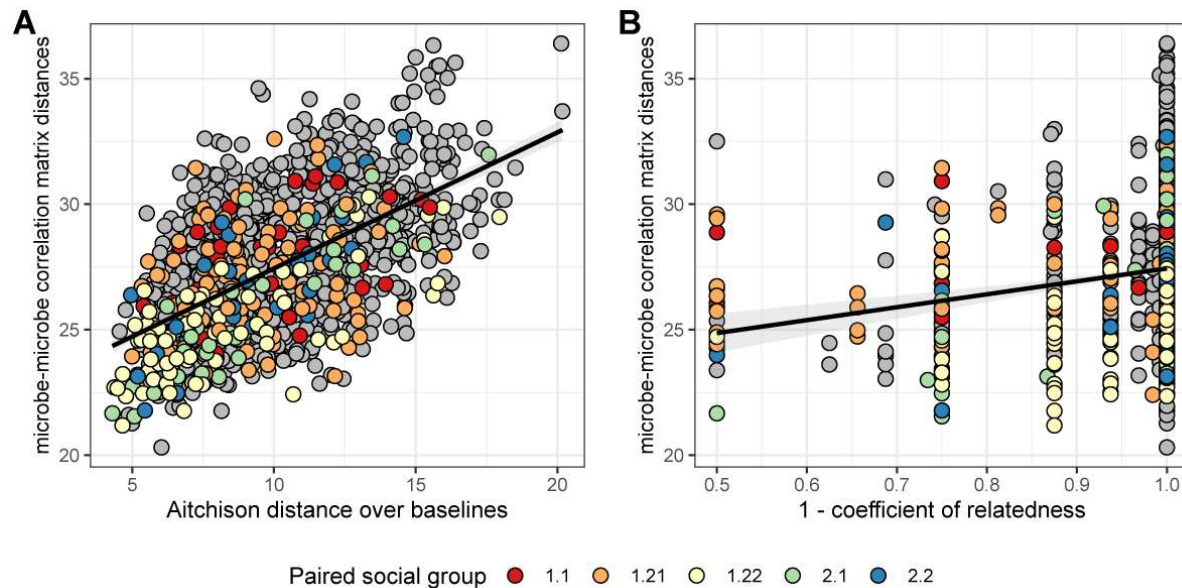
11

371 interquartile ranges for a given interval of phylogenetic distance. Phylogenetic distance is
372 negatively correlated with universality score in positive pairs (Pearson's correlation for
373 positively associated ASV pairs=-0.213, p-value < 0.0001), and positively correlated with
374 universality score in negatively associated pairs (Pearson's correlation for negatively associated
375 ASV pairs=0.049, p = 0.004). Panel **(C)** shows families for the ASV pairs enriched in the closest
376 related (distance < 0.2) and highly universal (score > 0.5) pairs. Panel **(D)** shows enriched
377 family-family pairings for the same subset of closely related and highly universal ASV pairs in
378 panel C. Note that for visualization, the estimated log2 odds ratio intervals have been truncated
379 at 5, which excludes 5 pairs with high uncertainty in the odds ratio; full estimates are given in
380 **Table S6.**
381
382

Genetic relatives, and hosts with similar microbiome compositions, have more similar bacterial correlation patterns

385 We next asked whether host-level variables, including sex, social group membership,
386 genetic relationships, and baseline gut microbiome composition predict host differences in
387 patterns of bacterial correlation. Consistent with prior research [10], the strongest predictor of
388 distance in bacterial correlation patterns was distance in terms of baseline microbiome
389 composition. Indeed, a Mantel test correlating compositional distance of average microbial
390 profiles (as Aitchison distances between the per-host mean of centered log-ratio-transformed
391 samples) with distance in microbial correlation patterns between hosts (via Frobenius distance)
392 revealed that 34% of the variation in correlation patterns was explained by baseline microbiome
393 community composition (Mantel: r^2=0.343; p=0.001; **Fig. 5A**; **Table S7**).
394 Consistent with prior research in our population, which finds widespread heritability of
395 the abundance of individual gut microbiome taxa [43], we also found a weak but significant
396 relationship between host genetic distance and the distance in microbial correlation patterns
397 between hosts. Hosts who were more distantly related based on a multigenerational pedigree
398 have slightly less similar ASV-level correlation matrices, as measured by Frobenius distance
399 (**Fig. 5B**; **Table S7**; r^2=0.025; Mantel p-value=0.001). We found no evidence that members of
400 the same social group or sex exhibit especially similar microbial correlation patterns (social
401 group: F=1.994; p=0.106; sex: F=1.784; p=0.187; **Table S7**).

Figure 5. Baboons with more similar bacterial correlation patterns are more likely to have more similar baseline microbiome compositions and are more likely to be genetic relatives. In panel **(A)** each point is a pair of hosts; the y-axis shows the similarity of these hosts' bacterial correlation patterns (via Frobenius distance) as a function of their microbiome compositional similarity (via Aitchison distance; Mantel: $r^2=0.343$; p=0.001). Colors show samples from pairs of baboons living in the same social group and grey dots are pairs of animals living in different social groups; there is no detectable effect of social group on correlation pattern similarity. Panel **(B)** shows the same Frobenius distances as a function of host genetic dissimilarity (1 – the coefficient of genetic relatedness between hosts; $R^2=0.025$; p-value Mantel test 0.001). Colors reflect pairs of hosts living in the same social group, as in panel A.

Universality in Amboseli is not solely explained by seasonality or synchrony

Without experiments, we cannot disentangle whether our observed bacterial correlations are due to ecological interactions between bacterial species (e.g., mutualisms, direct or indirect competition etc.) or to shared responses to environmental gradients. While our modeling approach accounts for seasonal changes in the first three principal components of the baboons' diets, to identify other potential effects of season we re-estimated the ASV-ASV correlation matrix after removing an oscillating seasonal trend from the observed log-ratio abundance for each ASV (**Fig. S8**). Removing this trend had little effect on the ASV-ASV correlation matrix; the variance explained by the seasonal oscillation is small for all ASVs (median 1.1%, minimum=0%, maximum=6%) and the between-ASV correlation estimates were almost identical to those derived from our original model (Pearson's r=0.979, p<0.0001; **Fig. S8C**). We also tested whether pairs of ASVs with especially consistent between-host correlation patterns tend to show large seasonal changes in CLR abundance. To do so, we focused on 13 families that exhibit significant seasonal changes in CLR abundance, based on a previous analysis of the same data set [42]. While ASV pairs in which one member belongs to one of these significantly "seasonal" families are slightly more universal, this effect is small (difference of 0.026, p<0.0001 vs. pairs where 0 or 1 partner were "seasonal"; **Fig. S9**).

13

433   Because the high level of universality we observed was not well explained by season, we
434   also tested whether universality is explained by synchronized dynamics. We reasoned that if one
435   member of an ASV pair shows highly synchronized dynamics across different hosts, and the
436   other member is also strongly synchronized across hosts, then universality could be an inevitable
437   outcome of each member of the pair's strong synchrony. We quantified synchrony as the degree
438   to which the observed dynamics of a single, focal ASV are consistent across hosts, such that high
439   synchrony (near 1) implies that the timing and direction of shifts in log-ratio ASV abundance are
440   identical across hosts in the population (see Methods; **Fig. S10**). Estimates of synchrony ranged
441   from 0.019 to 0.477 (median=0.196). Interestingly, ASVs in the 13 "seasonal" families are not
442   more likely to have high synchrony than other families (ANOVA, p=0.358; **Fig. S11**). However,
443   the average synchrony of an ASV-ASV pair did predict that pair's universality score (r=0.264,
444   p<0.0001): ASV pairs that are more synchronous on average are also more likely to show
445   consistent correlations across hosts. These high synchrony, high universality pairs are highly
446   enriched for Bifidobacteriaceae-Bifidobacteriaceae and Lachnospiraceae-Lachnospiraceae
447   family pairs (**Fig. S12**).
448
449   **Baboon microbiomes are not substantially more "universal" than human microbiomes**
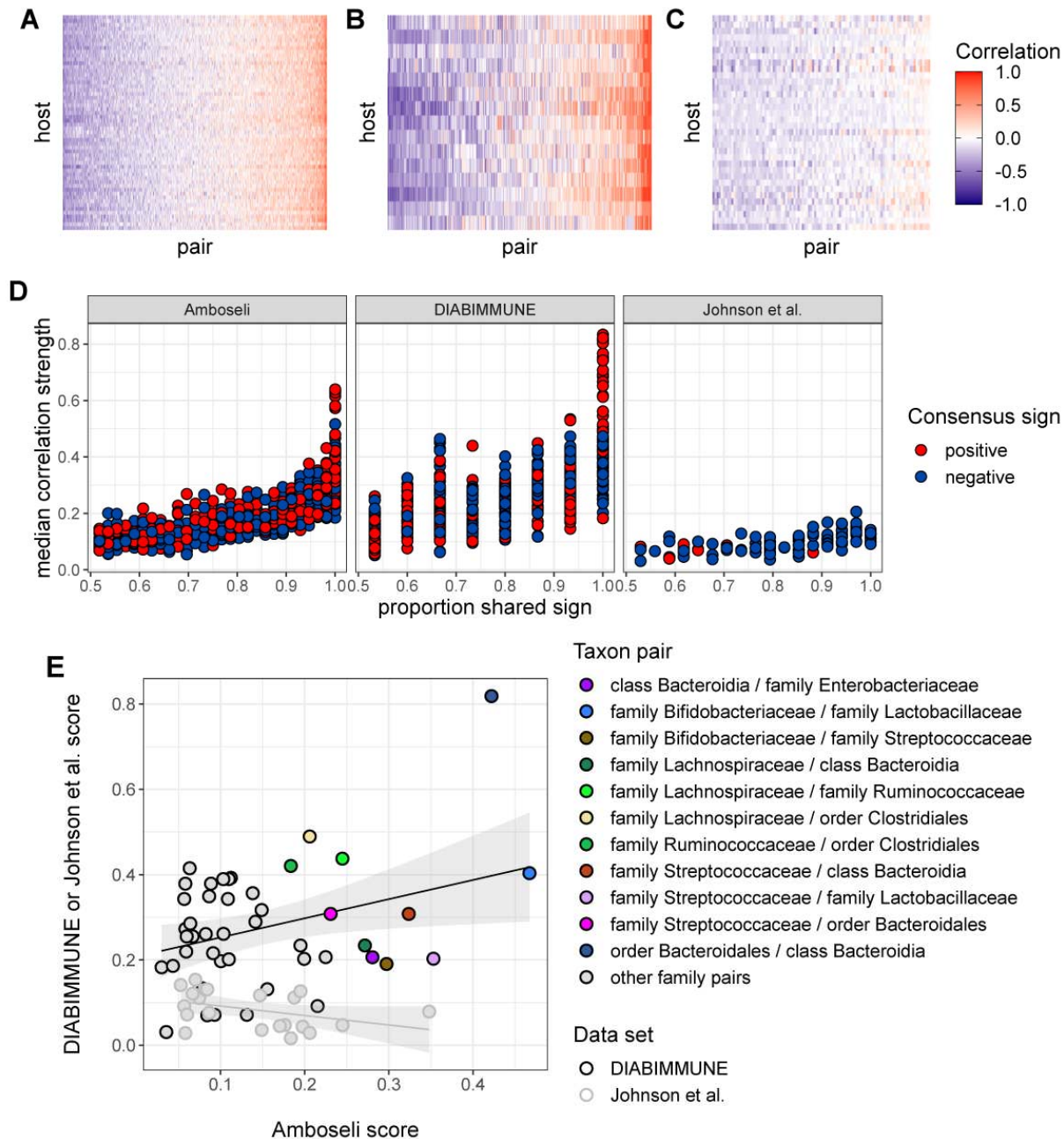450   Finally, to investigate the generalizability and applicability of our observations in
451   baboons, we turned to two publicly available gut microbial time-series data sets: daily samples
452   from 34 adults over a 17-day span (483 total samples; hereafter "Johnson et al." [34]), and the
453   DIABIMMUNE cohort that consists of 285 samples, collected monthly over 3 years, from 15
454   infants and toddlers living in Russian Karelia ([44; at the time of writing, these cohorts were the
455   only publicly available data sets we could find that included large numbers of repeated samples
456   from the same subjects). Because baboons in Amboseli experience less heterogeneity in their
457   environments and diets than humans [42, 43], we expected they would exhibit greater
458   consistency in microbial correlations than either human cohort. Note that we compared each host
459   cohort's universality at the family/order/class level because this taxonomic level offered the
460   greatest comparative power (10.1% of families/orders/classes overlap between the cohorts
461   compared to just 3.1% of genera and no ASVs).
462   Contrary to our expectations, we find comparable evidence of universality in baboons
463   and the DIABIMMUNE infant/toddler cohort, but weak universality in Johnson et al. (**Figs. 6A-
464   6D**). Bacterial families in the DIABIMMUNE cohort yielded universality scores slightly higher
465   than those observed in Amboseli (25th percentile=0.132, median=0.206, 75th percentile=0.316
466   for DIABIMMUNE; 25th percentile=0.088, median=0.150, 75th percentile=0.234 for
467   Amboseli), driven by relationships between families that were stronger on average than those
468   estimated for baboons (median DIABIMMUNE family-family correlation strength=0.270;
469   median Amboseli family-family correlation strength=0.181). The high level of consistency
470   between both infants/toddlers and baboons in one wild population is surprising and may point to
471   the similar sampling intervals for these cohorts. Both cohorts were sampled approximately
472   monthly, while Johnson et al.'s subjects were sampled daily [17, 48]. Median correlation
473   strengths and universality scores for the Johnson et al. [34] cohort were substantially lower
474   (median correlation=0.099; 25th percentile universality=0.050, median=0.076, 75th
475   percentile=0.111) than the DIABIMMUNE cohort or the baboons.
476   Despite considerable differences in the hosts, time scales, and designs of these studies, all
477   three data sets exhibited a positive correlation between correlation strength and sign consistency
478   for family pairs (**Fig. 6C**). This correlation was strongest in the Amboseli baboons (Spearman's

479   r=0.844; p<0.0001); weaker in the DIABIMMUNE cohort (r=0.686; p<0.0001) and weakest in
480   Johnson et al. [34] (r=0.644; p<0.0001). Further, the observation that the most universal family-
481   family associations skew positive in baboons was replicated in the infant data set, but not in
482   Johnson et al. [34]. All of the top 1% and top 2.5% most universal family pairs (6 of 6 and 16 of
483   16 pairs, respectively) are positively associated in the DIABIMMUNE cohort, compared to 86%
484   and 71% of these pairs in the Amboseli baboons.
485   Finally, we examined the relationship between universality scores for family pairs that
486   overlapped between Amboseli and DIABIMMUNE (n=45 pairs), and between Amboseli and
487   Johnson et al. [34] (**Fig. 6D**; n=21 pairs; only 10 family pairs overlapped between all three data
488   sets). For these overlapping pairs, scores in the Amboseli data predicted scores for the same
489   family-family pair in the DIABIMMUNE data set (r=0.449, p=0.023). The association between
490   scores in the Amboseli data and the Johnson et al. data was negative, but not statistically
491   significant (r=-0.222, p=0.071).

Figure 6. Patterns of universality in baboons are recapitulated in the DIABIMMUNE study. Following **Fig. 2A**, Panels **(A)**, **(B)**, and **(C)** show the Pearson's correlation coefficients of CLR abundances between all pairs of families (x-axis) in two time series data sets from human subjects: **(A)** the Amboseli baboons, **(B)** the DIABIMMUNE cohort, consisting of 15 infants/toddlers sampled monthly over 3 years in Russian Karelia [44], and **(C)** the diet study of Johnson et al. [34], including 34 adults sampled daily over 17 days. Following **Figs. 3A and B**, panel **(D)** shows the median correlation strength of each family pair's correlation coefficient across hosts as a function of the consistency in direction of that pair's correlation across hosts (i.e., the proportion of hosts that shared the majority correlation sign, positive or negative). Median correlation strength is low overall in Johnson et al. (median=0.099), whereas the

16

504   Amboseli baboon and DIABIMMUNE infant/toddler cohorts show similar relationships between
505   median correlation strength and the proportion shared correlation sign across hosts (Spearman's r
506   in Amboseli=0.844; Spearman's r in DIABIMMUNE=0.686). **(E)** Universality scores for
507   overlapping family pairs from the infant/toddler subjects of the DIABIMMUNE study and
508   baboons in the Amboseli study are significantly correlated (r=0.449, p=0.0226). Panel D shows
509   universality scores for overlapping gut bacterial family pairs in the Amboseli baboon and
510   DIABIMMUNE infant/toddler data sets (black outlines), as well as the Amboseli and Johnson et
511   al. data sets (gray outlines) on opposing axes. Color represents the taxonomic identities of the
512   family pairs.
513
514

515   **Discussion**
516   Do different hosts have different microbiome "ecologies"? Answering this question is
517   essential for predicting gut microbiome community assembly and dynamics, and for
518   understanding the degree to which the species interactions that govern these processes are shared
519   across hosts. Here, we overcome the constraints of previous cross-sectional analyses by
520   measuring bacterial correlations directly from longitudinal, multi-host microbiome time series.
521   Our results provide independent confirmation for prior studies that tested for universal gut
522   microbial relationships via dissimilarity overlap analyses (DOA; [10, 18-20, 36]). We confirm
523   that bacterial correlation patterns are largely shared across hosts in the same population, as
524   opposed to idiosyncratic to individual hosts, and that hosts with the most similar bacterial
525   correlation patterns are those with the most similar baseline microbiome compositions—a core
526   assumption of DOA. Because prior analyses of these microbiome time series find that each
527   baboon exhibits a highly personalized microbiome composition and dynamics [42], our findings
528   suggest that such compositional personalization, which is also common in humans [22-26, 31-
529   35], cannot be easily explained by personalized microbiome ecologies. Further, in terms of
530   microbiome therapeutics, our results suggest that widely applicable microbiome interventions
531   may be more attainable than personalized microbiome compositions would suggest.
532   By measuring bacterial correlations in multiple hosts, we were also able, for the first
533   time, to pinpoint which pairs of bacterial taxa exhibit the most consistent relationships across
534   hosts. Surprisingly, we found that the most universal bacterial pairs are almost always positively
535   (as opposed to negatively) correlated. Positive bacterial interactions have been the subject of
536   recent controversy [9, 15, 49]. Ecological theory predicts that strong positive interactions should
537   be rare in natural communities because species interdependencies can hamper community
538   assembly and stability [14, 17]. This theory is supported by experiments that directly measure the
539   effects of one bacterial species on another's growth [50-53] (but see [49]). Our results suggest
540   that positive bacterial correlations are indeed uncommon in intact, unmanipulated microbiomes:
541   significant positive relationships made up just 8.8% of all of the pairwise correlations we
542   observed. However, when they occur, they often contain taxa that belong to the same bacterial
543   families or are otherwise phylogenetically close, suggesting they may be members of the same
544   ecological guild and respond similarly to shared resources and other environmental drivers. This
545   pattern may partly explain the abundance of positively associated Lachnospiraceae pairs in our
546   data, a family in which positive, within-family interactions are known to contribute to
547   hydrolyzing starch and other complex carbohydrates, and ultimately the regulation of short chain
548   fatty acids (SCFAs) [54-56].

549   These observations—that bacterial correlation patterns are largely consistent across hosts,
550 and that the most consistent correlations are typically positive—were also apparent in one human
551 data set, despite differences in study design, host age, and time scale. Specifically, both the
552 Amboseli baboons and the DIABIMMUNE infant/toddler cohort from Russia [44] exhibit
553 comparable levels of universality. This outcome was surprising, given that baboons are expected
554 to experience less heterogeneity in their environments and diets than human children from birth
555 to age three years—even if those infants are from the same population (Russian Karelia). We
556 also found that the most universal bacterial families in baboons tended to be highly universal in
557 human infants/toddlers. Hence, some bacterial families may exhibit consistent microbial
558 relationships within hosts, across host populations, and across host species. Finally, a recent,
559 independent study also identified consistent bacterial correlation patterns across four different
560 populations of human hosts [9]. While this study lacked resolution at the level of individual
561 hosts, it did identify a highly conserved network of positively associated and closely related
562 microbes similar to those we identify in **Fig. 3**. The authors speculate that these conserved
563 associations may indicate strong partner fidelity or obligate partnerships.
564   We did, however, fail to detect universality in a second human data set reported in
565 Johnson et al. [34], in which subjects were sampled daily, rather than weekly or monthly. The
566 lack of universality in Johnson et al. [34] may be due to this difference in sampling time scale,
567 especially if daily abundances and correlations are noisier than covariances modeled over the
568 longer time scales in our study. In support, many fewer of the microbial correlations were
569 stronger than random chance in Johnson et al. as compared to the baboons or children in the
570 DIABIMMUNE cohort. The subjects in Johnson et al. [34] also consumed substantially different
571 diets from each other, perhaps more so than the children in the DIABIMMUNE cohort, and this
572 inter-host difference in diet may reduce the universality of microbial correlations.
573   In terms of understanding microbiome ecology, an essential caveat to our findings is that
574 the correlation patterns we observed could reflect either direct or indirect relationships, or
575 uncontrolled environmental gradients, and they cannot be mapped directly to standard categories
576 of pairwise ecological interactions, such as mutualism, commensalism, amensalism, exploitation,
577 or competition. Experimental approaches that directly measure the effects of one species on
578 another's growth *in vitro* are better suited to characterizing these relationships [49-53]. However,
579 even then, caution is required because a microbe's community and environmental context can
580 have important consequences for its metabolism, functional capacities, and relationships with
581 other microbes. We surmise that most of the correlation patterns we observed are not attributable
582 to environmental gradients because our signature of universality persisted, even when we
583 accounted for diet, oscillating seasonal drivers, and microbial synchrony between hosts. Hence,
584 some of correlations we observed may derive from microbial interactions themselves, rather than
585 shared environmental drivers creating shared dynamics.
586   Our finding that correlations between gut microbial taxa are largely consistent across
587 hosts is important, considering that many studies find highly personalized gut microbial
588 compositions and single-taxon dynamics [27-29]. Personalized compositions and dynamics in
589 the gut microbiome are commonly attributed to horizontal gene transfer and functional
590 redundancy, which may lead some bacteria to perform different functions and exhibit different
591 environmental responses in different hosts. Our results suggest these processes do not
592 substantially alter pairwise microbial associations in the gut, at least for highly prevalent taxa at
593 the level of ASVs and above, and on the time scales in our study (on the order of weeks and
594 months). Because ASVs encompass multiple species and strains, reflecting the functional

18

595   diversity of these taxa, their dynamics may be somewhat buffered against idiosyncrasies driven
596   by horizontal gene transfer and functional redundancy, which affect single strains more strongly
597   than whole species or genera. If so, personalized gut microbial compositions may emerge instead
598   from personalized assembly processes [57, 58], the fact that most microbial relationships are
599   weak, and the effects of rare, host-specific taxa (which were necessarily excluded from our
600   analyses). A logical next step would be to confirm the stability of the microbial correlations we
601   observed using culture-based approaches, which will help reveal the stability of these
602   correlations in vitro and whether they can be attributed to direct effects of one microbe on
603   another's growth.
604
605   **Methods**
606   **Study population and microbiome profiles**
607   The baboon hosts in this study were members of the Amboseli baboon population, which
608   has been studied by the Amboseli Baboon Research Project since 1971 [41]. The microbiome
609   compositional profiles are derived from V4 16S rRNA gene amplicon sequencing data that were
610   previously analyzed in [42, 43]. Our analyses use 5,534 of these profiles from 56 especially well-
611   sampled baboons, collected over a 13.3-year span between 2000 to 2013 (**Fig. 1B**). Each baboon
612   host in this data set was sampled at least 75 times (mean number of samples=99; range=75 to
613   181 samples; median number of days between samples within hosts=20 days; 25th percentile=7
614   days, 75th percentile =49 days). DNA was extracted from each sample using the MoBio and
615   QIAGEN PowerSoil kit with a bead-beating step. All samples were sequenced on an Illumina
616   HiSeq 2500, with a median read count of 48,827 reads per sample across all 5,534 samples
617   (range=982 to 459,315 reads per sample). Further details of sample collection, DNA extraction,
618   and sequencing can be found in [42, 43].
619
620   **Filtering of low-abundance taxa**
621   Data sets of per-sample taxonomic counts were produced at each of three taxonomic
622   levels, from finest to coarsest: ASV, taxonomic assignments finer than phyla, but above the
623   genus level (e.g., class, order, family), and phylum. At the intermediate and coarsest levels, taxa
624   were agglomerated using phyloseq's tax_glom() function [59] such that all sequence variants
625   sharing taxonomic identity at that level were collapsed into a single taxon (e.g. family
626   Bifidobacteraceae).
627   To reduce sparsity in the data set, remove 16S sequences that could represent gene
628   duplications, and focus only on taxa that were prevalent in all 56 hosts, we further filtered as
629   follows: (1) in each of the three taxonomically defined data sets (i.e. ASV, taxa assigned to
630   family/order/class, and phylum), we identified taxa present in a minimum of 20% of each host's
631   samples; (2) if a given ASV was >99% genetically similar to another ASV we removed the least
632   abundant of the pair to minimize the risk of including duplicate 16S rRNA gene copies from the
633   same taxa [47]; and (3) counts associated with all other taxa were combined into a dummy
634   category, hereafter referred to as "other." The "other" category therefore includes a combination
635   of rare and host-specific gut microbes. This category was retained in the data set (although not
636   analyzed directly) because "other" counts still inform the precision of the observed relative
637   abundances in our model. Characteristics of the filtered data at each taxonomic level are
638   provided in **Tables S1-S3**.
639
640

19

Modeling log-ratio dynamics

Estimates of taxon-taxon covariance were obtained from the *basset* model of the "fido" package in R [46]. Data for each host took the form of a $D \times N$ count matrix, where D gives the number of taxa and N the number of samples collected for a given host. The following model was fit to each host's count matrix (Y) where Y_i represents the counts associated with a single sample:

$$Y_i \sim \text{Multinomial}(\pi_i)$$
$$\pi_i = \text{ALR}^{-1}(\eta_i)$$
$$\eta \sim \text{Normal}(\Lambda, \Sigma, I)$$
$$\Lambda \sim \text{GP}(\Theta[X], \Sigma, \Gamma[X])$$
$$\Sigma \sim \text{inv-Wishart}(\Xi, \nu)$$

The observed relative abundances are considered to be drawn from a multinomial distribution parameterized by a set of proportions (π) which have an analogous representation in the additive log-ratio. The dynamics of these log-ratio abundances (η) are described by what amounts to a state space model in the 3$^{\text{rd}}$ and 4$^{\text{th}}$ lines of the specification above, where a Gaussian process models the evolution of a "latent" state. The matrix Σ captures covariation in log-ratio abundances (the D rows of the observed count matrix). Sample-sample covariation arising from nearness in time (autocorrelation) is modeled by the kernel matrix Γ. Both the kernel matrix and the expected baseline log-ratio abundances (Θ) are parameterized by a set of time-varying covariates X which included the day of sampling (where the date of first sample is defined as zero) and the first three principal components of diet composition, calculated following [42, 43] as the diet all juveniles and females living in the host's social group in the 30 days prior to sample collection. All group members consume highly similar diets as they travel in a together across the habitat, encountering the same resources at the same time [42, 43]. These data are collected via random-order behavioral observations collected two to four times per week on adult females and juveniles in each social group. Parameterization of the kernel matrix is further described in the Supplement.

Posterior inference on this model is performed as described in [46] and yields estimates of the distributions of parameters necessary to reconstruct trajectories for all log-ratio taxa across sampling time. In particular, we extract the posterior estimates of one such parameter, Σ, the covariance of additive log-ratio (ALR) taxa, from the fitted models for each host. We convert these covariance matrices over ALR taxa to the centered log-ratio (CLR) form (a simple linear transformation of the matrix). We then normalize estimated CLR covariance matrices to Pearson correlation matrices in R using the built-in cov2cor() function.

Calculating universality scores for taxon-taxon pairs

We devised a universality score for each pair of taxa intended to capture the strength and consistency of taxon-taxon correlations across hosts. The majority direction is negative otherwise. This score identifies the sign of the taxon-taxon correlation (positive or negative) that is most common across the 56 hosts (i.e., occurs in >50% of the 56 hosts in the data set). The direction of this sign is the "majority correlation sign."

For a pair of taxa i, let n_i^{maj} be the number of hosts with CLR correlation over pair i with the majority correlation sign for that pair and let n be the total number of hosts. Let R be the

20

681 subset of estimated CLR correlations for pair i across hosts with the majority sign. The
682 universality score u_i for that taxon-taxon pair is then given by
683

$$u_i = \frac{n_i^{\text{maj}}}{n} \times \text{median}(R)$$

684
685   This score is the product of the median CLR correlation across hosts and the proportion
686 of hosts with the majority correlation sign, and is bounded between 0 and 1. Scores near 1
687 indicate strong universality and near-zero scores indicate weak universality. Strong universality
688 can only be achieved by taxon-taxon correlations that are both large in magnitude and highly
689 concordant across hosts.

690
691 **Defining a cutoff for significant bacterial correlations and universality scores**
692   We identified correlations stronger than expected under random simulations using
693 permutations of the data set to define empirical null distributions (**Fig. S4A**). Specifically, we
694 permuted the data by randomly shuffling taxon identity within each sample 10 times for each of
695 the 56 hosts. This procedure maintained relative abundance patterns within a sample but
696 scrambled the covariance patterns of relative abundances. The distributions of ASV-level CLR
697 correlations in the original and permuted data are shown in **Fig. S4A**. We identified "significant"
698 correlations as those below FDR ≤ 0.05 (Benjamini-Hochberg), testing against the permuted
699 data.
700   We applied an analogous permutation test to derive a null distribution for taxon-taxon
701 universality scores. In a single iteration of this permutation procedure, rows and columns of the
702 observed taxon-taxon correlation matrix for each host were shuffled, maintaining the distribution
703 over observed correlations at the host level but randomizing the identity of taxon pairs across
704 hosts. This procedure was repeated 100 times and universality scores were calculated from each
705 of these shuffled data sets to give a pseudo-null distribution of universality scores. The observed
706 and null distributions of universality scores at the ASV level are shown in **Fig. S4B**. We used
707 this empirical null distribution to identify universality scores significantly greater than expected
708 (FDR ≤ 0.05).

709
710 **Estimating the ratio of population-level to host-level contributions to observed taxon-taxon**
711 **correlation patterns**
712   We used simulations to estimate the degree of shared "signal" between hosts in terms of
713 taxon-taxon correlations. Each host's "observed correlations" were defined as the *basset*
714 estimated maximum a posteriori (MAP) estimates of centered log-ratio ASV correlations for that
715 host. We computed the *mean* correlations across the population using the function estcov() from
716 the shapes package in R [60] and estimated a host-specific contribution to the observed
717 correlations as the residual *difference* between per-host observed and these mean correlations.
718 That is,
719

        observed host correlations = mean population correlations + host residual

720
721   For each host, we simulated a hypothetical set of composite taxon-taxon correlations as a
722 convex combination of mean and host residual:
723

$$\text{composite correlations} = (1 - \alpha) \times \text{mean population correlations} + \alpha \times \text{host residual}$$

724

725   A cartoon example of this procedure is given in **Fig. S7A**. For example, one such
726 simulated set of taxon-taxon correlations might constitute a mixture of 90% host contribution
727 and 10% shared population-level "signal" ($\alpha=0.9$). Alternatively, a small host-level contribution
728 might have $\alpha=0.1$.
729   For each host, we iterated over increasing proportions of host-level contribution (from
730 0% to 100%), generating simulated composite correlation matrices according to the formula
731 above. We compared these simulated patterns to those observed for the same host, reasoning that
732 simulated correlation matrices that minimize the distance between the observed correlation
733 matrices and the simulated mixtures provide the best description of the underlying true mixture.

734

735 **Estimating synchrony**
736   Seasonal autoregressive models were fit independently to each CLR-transformed ASV
737 with arima() in R, using covariate matrices which included per-host intercepts and an oscillating
738 periodic trend to mimic wet-dry season oscillation. For each ASV, all hosts' samples were
739 combined into a single series, yielding per-ASV models of CLR dynamics. This procedure is
740 detailed in the Supplemental Methods. Residuals were extracted from these fitted models as
741 seasonally "de-trended" data and CLR correlation matrices across ASV pairs were estimated
742 directly from these adjusted data using cov() in R (**Fig. S9**).
743   "Synchrony" was estimated by sampling aligned microbiome compositional profiles
744 across hosts. We identified all samples collected from pairs of hosts within 1 calendar day. For
745 instance, a sample collected from host F01 on 2011-03-14 could pair with a sample from M04 on
746 2011-03-15. For all possible pairs of hosts, we selected one such aligned pair of samples,
747 yielding 1540 joint observations of gut microbiome composition. For each such paired sample,
748 one host was arbitrarily designated as host A and the other as host B. The "synchrony" of a given
749 taxon was estimated as the correlation of a taxon's model-inferred log-ratio abundance across the
750 set of samples from hosts labeled A and the set of samples from hosts labeled B. The cartoon in
751 **Fig. S10** illustrates this sample pairing.

752

753 **Enrichment analyses**
754   We performed enrichment analyses for bacterial families and family pairs in several
755 settings. In each case we computed the frequency of ASVs belonging to a given family, or of
756 pairs belonging to a family pair, on a subset of the data. These were compared to the overall
757 frequencies of ASVs belonging to those families or pairs.
758   To determine the enrichment of families and family pairs in the most universal ASV pairs
759 (**Fig. 3E and 3F**), we calculated the frequencies of ASV families and pairs in the top 2.5% of
760 pairs by universality scores. Significant enrichment of families or pairs was identified using a
761 one-sided Fisher's Exact Test. Multiple test correction was applied as a Benjamini-Hochberg
762 adjustment to observed p-values.
763   Phylogenetic distances between ASV sequences were calculated with the dist.ml function
764 in the "phangorn" package in R [61] using default settings for amino acid substitution rates. In
765 **Fig. 4C and 4D**, low phylogenetic distance/high median correlation strength pairs were
766 identified as those with phylogenetic distances of less than 0.2 and median correlation strengths
767 of greater than 0.5. Again, significance of these was evaluated against overall frequencies of the
768 same families and pairs.

769   To determine enrichment of low synchrony/high universality or of high synchrony/high
770   universality families and pairs (shown in **Fig. S12A and 12B**), we defined the low
771   synchrony/high universality cohort as those ASV pairs with synchrony estimates of less than 0.3
772   and universality estimates greater than 0.4. We defined the high synchrony/high universality
773   cohort as those ASV pairs with synchrony greater than 0.3 and universality greater than 0.4. The
774   frequency of these subsets was evaluated against the overall frequencies of the same families and
775   pairs.
776
777   **Evaluating explanatory factors**
778   *Variation in taxon-taxon correlation patterns explained by kinship and baseline*
779   *composition*. To evaluate a possible explanatory effect of distances in terms of kinship or
780   baseline gut bacterial composition on distances in terms of taxon-taxon correlation patterns, we
781   applied Mantel tests. However, because population structure can lead to anticonservative p-
782   values [62], we also developed a second simulation-based procedure for evaluating the
783   significance of baseline composition, using a permutation procedure of our own design. Firstly,
784   baseline composition for each host was estimated by transforming all of a given host's samples
785   to the centered log-ratio representation after adding a small fraction (0.5) to remove zeros. The
786   vector of per-taxon averages of these CLR values was used as that host's "baseline" CLR
787   composition. The Euclidean distances between hosts in terms of these per-host baselines were
788   compared against distances in terms of correlation patterns to give an r^2 value.
789   In the case of the customized permutation test, this observed result was evaluated against
790   a pseudo-null distribution computed in the following way. The identity of each taxon in the
791   baseline composition was shuffled for each host independently. Euclidean distances across these
792   shuffled baselines were computed and an r^2 value calculated for these distances against the
793   observed distances computed from taxon-taxon correlation patterns. This procedure was repeated
794   1000 times to give a distribution of "random" r^2 values we used as an empirical null.
795   *Variation in taxon-taxon correlation patterns explained by sex and social group*. To test
796   whether host sex or social group membership predicted similarity in terms of correlation
797   patterns, we used an ANOVA-like strategy. We calculated the F-statistic, a ratio of between- to
798   within-group variation, on the observed correlation patterns (strictly, the vectorized CLR taxon-
799   taxon correlation matrices; Z in the equation below) and segmented samples into groups defined
800   by either sex or social group. The F-statistic was calculated as
801

$$F = \frac{\text{between-group variation}}{\text{within-group variation}} = \frac{\sum_{i=1}^{K} n_i (\bar{Z}_i - \bar{Z})^2 / K - 1}{\sum_{i=1}^{K} \sum_{j=1}^{n_i} (Z_{ij} - \bar{Z}_i)^2 / (N - K)}$$

802
803   and significance was evaluated via an F-distribution parameterized by the appropriate degrees of
804   freedom. Here K represents the number of groups (e.g. two, in the case of sex) and N, the total
805   number of hosts. The matrix $\bar{Z}_i$ consists of the mean taxon-taxon correlations for group i and $\bar{Z}$,
806   the population mean correlations.
807
808   **Comparison to microbiome time series from human populations**
809   We compared our findings to those generated from two human data sets: the
810   DIABIMMUNE project's infant/toddler cohort from Russian Karelia [44] and the adult diet-
811   microbiome association study of Johnson et al. [34]. In both cases, count tables were obtained
812   from the project's public website and subject identity and sampling schedules were available in

23

813   the associated metadata. We compared each host cohort's universality at the family/order/class
814   level because this taxonomic level offered the greatest comparative power (10.1% of
815   families/orders/classes overlap between the cohorts compared to just 3.1% of genera and no
816   ASVs). The *basset* model from the "fido" R package [46] was fit to each subject's data set using
817   model settings analogous to those employed on the Amboseli baboon series: first, only taxa with
818   non-zero counts in at least 20% of all subjects' series were retained; second, Gaussian process
819   kernel bandwidth settings were chosen in such a way as to encode an expectation of minimum
820   autocorrelation between samples at a distance in time of 90 days. We extracted centered log-ratio
821   estimates of taxa at the family level in the same manner as described previously for the Amboseli
822   data set.

823

852

853   **Data and code availability**
854   16S rRNA gene sequences are available on EBI-ENA (project 590 ERP119849) and Qiita
855   (study 12949). Analyzed data and code is available on GitHub at:
856   https://github.com/kimberlyroche/rulesoflife

857

858

References

1. Faust K, Raes J. Microbial interactions: from networks to models. Nature Reviews Microbiology. 2012;10(8):538-50. doi: 10.1038/nrmicro2832. PubMed PMID: 22796884.

2. Foster KR, Bell T. Competition, Not Cooperation, Dominates Interactions among Culturable Microbial Species. Current Biology. 2012;22(19):1845-50. doi: 10.1016/j.cub.2012.08.005. PubMed PMID: WOS:000309792900031.

3. Dolinsek J, Goldschmidt F, Johnson DR. Synthetic microbial ecology and the dynamic interplay between microbial genotypes. Fems Microbiology Reviews. 2016;40(6):961-79. doi: 10.1093/femsre/fuw024. PubMed PMID: WOS:000387995000010.

4. Seth EC, Taga ME. Nutrient cross-feeding in the microbial world. Front Microbiol. 2014;5:350. Epub 20140708. doi: 10.3389/fmicb.2014.00350. PubMed PMID: 25071756; PubMed Central PMCID: PMCPMC4086397.

5. Backhed F, Ley RE, Sonnenburg JL, Peterson DA, Gordon JI. Host-bacterial mutualism in the human intestine. Science. 2005;307(5717):1915-20. doi: Doi 10.1126/Science.1104816. PubMed PMID: ISI:000227957300045.

6. Gould AL, Zhang V, Lamberti L, Jones EW, Obadia B, Korasidis N, et al. Microbiome interactions shape host fitness. Proc Natl Acad Sci U S A. 2018. doi: 10.1073/pnas.1809349115. PubMed PMID: 30510004.

7. Pontrelli S, Szabo R, Pollak S, Schwartzman J, Ledezma-Tejeida D, Cordero OX, et al. Metabolic cross-feeding structures the assembly of polysaccharide degrading communities. Sci Adv. 2022;8(8):eabk3076. Epub 20220223. doi: 10.1126/sciadv.abk3076. PubMed PMID: 35196097; PubMed Central PMCID: PMCPMC8865766.

8. Degnan PH, Taga ME, Goodman AL. Vitamin B12 as a modulator of gut microbial ecology. Cell Metab. 2014;20(5):769-78. doi: 10.1016/j.cmet.2014.10.002. PubMed PMID: 25440056; PubMed Central PMCID: PMCPMC4260394.

9. Loftus M, Hassouneh SA, Yooseph S. Bacterial associations in the healthy human gut microbiome across populations. Sci Rep. 2021;11(1):2828. Epub 20210202. doi: 10.1038/s41598-021-82449-0. PubMed PMID: 33531651; PubMed Central PMCID: PMCPMC7854710.

10. Bashan A, Gibson TE, Friedman J, Carey VJ, Weiss ST, Hohmann EL, et al. Universality of human microbial dynamics. Nature. 2016;534(7606):259-62. doi: 10.1038/nature18301. PubMed PMID: 27279224; PubMed Central PMCID: PMCPMC4902290.

11. Widder S, Allen RJ, Pfeiffer T, Curtis TP, Wiuf C, Sloan WT, et al. Challenges in microbial ecology: building predictive understanding of community function and dynamics. ISME Journal. 2016;10(11):2557-68. doi: 10.1038/ismej.2016.45. PubMed PMID: 27022995.

12. Cao HT, Gibson TE, Bashan A, Liu YY. Inferring human microbial dynamics from temporal metagenomics data: Pitfalls and lessons. Bioessays. 2017;39(2):1600188. doi: 10.1002/bies.201600188. PubMed PMID: 28000336.

13. Faust K, Raes J. Host-microbe interaction: Rules of the game for microbiota. Nature. 2016;534(7606):182-3. doi: 10.1038/534182a. PubMed PMID: 27279206.

14. Coyte KZ, Schluter J, Foster KR. The ecology of the microbiome: Networks, competition, and stability. Science. 2015;350(6261):663-6. doi: 10.1126/science.aad2602. PubMed PMID: 26542567.

15. Palmer JD, Foster KR. Bacterial species rarely work together. Science. 2022;376(6593):581-2. Epub 20220505. doi: 10.1126/science.abn5093. PubMed PMID: 35511986.

16. Wu G, Zhao N, Zhang C, Lam YY, Zhao L. Guild-based analysis for understanding gut microbiome in human health and diseases. Genome Med. 2021;13(1):22. Epub 2021/02/11. doi: 10.1186/s13073-021-00840-y. PubMed PMID: 33563315; PubMed Central PMCID: PMCPMC7874449.

17. Coyte KZ, Rao C, Rakoff-Nahoum S, Foster KR. Ecological rules for the assembly of microbiome communities. PLoS Biol. 2021;19(2):e3001116. Epub 20210219. doi: 10.1371/journal.pbio.3001116. PubMed PMID: 33606675; PubMed Central PMCID: PMCPMC7946185.

18. Gao C, Montoya L, Xu L, Madera M, Hollingsworth J, Purdom E, et al. Fungal community assembly in drought-stressed sorghum shows stochasticity, selection, and universal ecological dynamics. Nat

910   Commun. 2020;11(1):34. Epub 2020/01/09. doi: 10.1038/s41467-019-13913-9. PubMed PMID:
911   31911594; PubMed Central PMCID: PMCPMC6946711.
912   19. Vila JCC, Liu YY, Sanchez A. Dissimilarity-Overlap analysis of replicate enrichment communities.
913   ISME J. 2020;14(10):2505-13. Epub 20200618. doi: 10.1038/s41396-020-0702-7. PubMed PMID:
914   32555503; PubMed Central PMCID: PMCPMC7490387.
915   20. San-Juan-Vergara H, Zurek E, Ajami NJ, Mogollon C, Pena M, Portnoy I, et al. A Lachnospiraceae-
916   dominated bacterial signature in the fecal microbiota of HIV-infected individuals from Colombia,
917   South America. Sci Rep. 2018;8(1):4479. Epub 20180314. doi: 10.1038/s41598-018-22629-7.
918   PubMed PMID: 29540734; PubMed Central PMCID: PMCPMC5852036.
919   21. Gonze D, Coyte KZ, Lahti L, Faust K. Microbial communities as dynamical systems. Current
920   Opinion in Microbiology. 2018;44:41-9. doi: 10.1016/j.mib.2018.07.004. PubMed PMID:
921   WOS:000447581000007.
922   22. Franzosa EA, Huang K, Meadow JF, Gevers D, Lemon KP, Bohannan BJM, et al. Identifying
923   personal microbiomes using metagenomic codes. Proceedings of the National Academy of Sciences.
924   2015;112(22):E2930-E8. doi: 10.1073/pnas.1423854112. PubMed PMID: WOS:000355832200014.
925   23. Faith JJ, Guruge JL, Charbonneau M, Subramanian S, Seedorf H, Goodman AL, et al. The long-term
926   stability of the human gut microbiota. Science. 2013;341(6141):1237439. Epub 2013/07/06. doi:
927   10.1126/science.1237439. PubMed PMID: 23828941; PubMed Central PMCID: PMC3791589.
928   24. Bik EM, Costello EK, Switzer AD, Callahan BJ, Holmes SP, Wells RS, et al. Marine mammals
929   harbor unique microbiotas shaped by and yet distinct from the sea. Nat Commun. 2016;7:10516.
930   Epub 20160203. doi: 10.1038/ncomms10516. PubMed PMID: 26839246; PubMed Central PMCID:
931   PMCPMC4742810.
932   25. Caporaso JG, Lauber CL, Costello EK, Berg-Lyons D, Gonzalez A, Stombaugh J, et al. Moving
933   pictures of the human microbiome. Genome Biology. 2011;12(5):R50. doi: Artn R50
934   Doi 10.1186/Gb-2011-12-5-R50. PubMed PMID: ISI:000295732700014.
935   26. Costello EK, Lauber CL, Hamady M, Fierer N, Gordon JI, Knight R. Bacterial community variation
936   in human body habitats across space and time. Science. 2009;326(5960):1694-7. doi: Doi
937   10.1126/Science.1177486. PubMed PMID: ISI:000272839000053.
938   27. Louca S, Polz MF, Mazel F, Albright MBN, Huber JA, O'Connor MI, et al. Function and functional
939   redundancy in microbial systems. Nat Ecol Evol. 2018;2(6):936-43. Epub 2018/04/18. doi:
940   10.1038/s41559-018-0519-1. PubMed PMID: 29662222.
941   28. Rainey PB, Quistad SD. Toward a dynamical understanding of microbial communities. Philos Trans
942   R Soc Lond B Biol Sci. 2020;375(1798):20190248. Epub 2020/03/24. doi: 10.1098/rstb.2019.0248.
943   PubMed PMID: 32200735; PubMed Central PMCID: PMCPMC7133524.
944   29. Martiny JB, Jones SE, Lennon JT, Martiny AC. Microbiomes in light of traits: A phylogenetic
945   perspective. Science. 2015;350(6261):aac9323. doi: 10.1126/science.aac9323. PubMed PMID:
946   26542581.
947   30. Debray R, Herbert RA, Jaffe AL, Crits-Christoph A, Power ME, Koskella B. Priority effects in
948   microbiome assembly. Nat Rev Microbiol. 2022;20(2):109-21. Epub 20210827. doi: 10.1038/s41579-
949   021-00604-w. PubMed PMID: 34453137.
950   31. Risely A, Wilhelm K, Clutton-Brock T, Manser MB, Sommer S. Diurnal oscillations in gut bacterial
951   load and composition eclipse seasonal and lifetime dynamics in wild meerkats. Nat Commun.
952   2021;12(1):6017. Epub 20211014. doi: 10.1038/s41467-021-26298-5. PubMed PMID: 34650048;
953   PubMed Central PMCID: PMCPMC8516918.
954   32. Kolodny O, Weinberg M, Reshef L, Harten L, Hefetz A, Gophna U, et al. Coordinated change at the
955   colony level in fruit bat fur microbiomes through time. Nature Ecology & Evolution. 2019;3(1):116-
956   24. doi: 10.1038/s41559-018-0731-z. PubMed PMID: WOS:000453767000021.
957   33. Flores GE, Caporaso JG, Henley JB, Rideout JR, Domogala D, Chase J, et al. Temporal variability is
958   a personalized feature of the human microbiome. Genome Biology. 2014;15(12):531. doi: ARTN 531
959   10.1186/s13059-014-0531-y. PubMed PMID: WOS:000346609500011.

960 34. Johnson AJ, Vangay P, Al-Ghalith GA, Hillmann BM, Ward TL, Shields-Cutler RR, et al. Daily
961   Sampling Reveals Personalized Diet-Microbiome Associations in Humans. Cell Host & Microbe.
962   2019;25(6):789-802. Epub 2019/06/14. doi: 10.1016/j.chom.2019.05.005. PubMed PMID: 31194939.
963 35. Smits SA, Marcobal A, Higginbottom S, Sonnenburg JL, Kashyap PC. Individualized Responses of
964   Gut Microbiota to Dietary Intervention Modeled in Humanized Mice. mSystems. 2016.
965 36. Kalyuzhny M, Shnerb NM. Dissimilarity-overlap analysis of community dynamics: Opportunities
966   and pitfalls. Methods in Ecology and Evolution. 2017;8:1764-73.
967 37. Marsland R, 3rd, Cui W, Mehta P. A minimal model for microbial biodiversity can reproduce
968   experimentally observed ecological patterns. Sci Rep. 2020;10(1):3308. Epub 20200224. doi:
969   10.1038/s41598-020-60130-2. PubMed PMID: 32094388; PubMed Central PMCID:
970   PMCPMC7039880.
971 38. Faust K, Lahti L, Gonze D, de Vos WM, Raes J. Metagenomics meets time series analysis:
972   unraveling microbial community dynamics. Current Opinion in Microbiology. 2015;25:56-66. doi:
973   10.1016/j.mib.2015.04.004. PubMed PMID: 26005845.
974 39. Gloor GB, Macklaim JM, Pawlowsky-Glahn V, Egozcue JJ. Microbiome datasets are compositional:
975   and this is not optional. Front Microbiol. 2017;8:2224. Epub 2017/12/01. doi:
976   10.3389/fmicb.2017.02224. PubMed PMID: 29187837; PubMed Central PMCID:
977   PMCPMC5695134.
978 40. Quinn TP, Richarrson MF, Lovell D, Crowley TM. propr: An R-package for Identifying
979   Proportionally Abundant Features Using Compositional Data Analysis Scientific Reports.
980   2017;7:16252.
981 41. Alberts SC, Altmann J. The Amboseli Baboon Research Project: Themes of continuity and change.
982   In: Kappeler P, Watts DP, editors. Long-term field studies of primates: Springer Verlag; 2012. p. 261-
983   87.
984 42. Bjo□rk J, Dasari M, Grieneisen L, Gould TJ, Grenier JC, Yotova V, et al. Synchrony and
985   idiosyncrasy in the gut microbiome of wild primates. Nature Ecology & Evolution. 2022;6:955-64.
986   doi: https://www.biorxiv.org/content/10.1101/2021.11.24.469913v1.
987 43. Grieneisen L, Dasari M, Gould TJ, Bjo□rk JR, Grenier JC, Yotova V, et al. Gut microbiome
988   heritability is near-universal but environmentally contingent. Science. 2021;373:181-6.
989 44. Vatanen T, Kostic AD, d'Hennezel E, Siljander H, Franzosa EA, Yassour M, et al. Variation in
990   Microbiome LPS Immunogenicity Contributes to Autoimmunity in Humans. Cell. 2016;165(4):842-
991   53. Epub 20160428. doi: 10.1016/j.cell.2016.04.007. PubMed PMID: 27133167; PubMed Central
992   PMCID: PMCPMC4950857.
993 45. Cullen CM, Aneja KK, Beyhan S, Cho CE, Woloszynek S, Convertino M, et al. Emerging Priorities
994   for Microbiome Research. Front Microbiol. 2020;11:136. Epub 2020/03/07. doi:
995   10.3389/fmicb.2020.00136. PubMed PMID: 32140140; PubMed Central PMCID:
996   PMCPMC7042322.
997 46. Silverman JD, Roche K, Holmes ZC, David LA, Mukherjee S. Bayesian Multinomial Logistic
998   Normal Models through Marginally Latent Matrix-T Processes. Journal of Machine Learning
999   Research. 2022;23:1-42.
1000 47. Vetrovsky T, Baldrian P. The variability of the 16S rRNA gene in bacterial genomes and its
1001   consequences for bacterial community analyses. PLoS One. 2013;8(2):e57923. Epub 20130227. doi:
1002   10.1371/journal.pone.0057923. PubMed PMID: 23460914; PubMed Central PMCID:
1003   PMCPMC3583900.
1004 48. Guittar J, Shade A, Litchman E. Trait-based community assembly and succession of the infant gut
1005   microbiome. Nat Commun. 2019;10(1):512. Epub 2019/02/03. doi: 10.1038/s41467-019-08377-w.
1006   PubMed PMID: 30710083; PubMed Central PMCID: PMCPMC6358638.
1007 49. Kehe J, Ortiz A, Kulesa A, Gore J, Blainey PC, Friedman J. Positive interactions are common among
1008   culturable bacteria. Science Advances. 2021;45:eabi7159.
1009 50. Weiss AS, Burrichter AG, Durai Raj AC, von Strempel A, Meng C, Kleigrewe K, et al. In vitro
1010   interaction network of a synthetic gut bacterial community. ISME J. 2022;16(4):1095-109. Epub

20211202. doi: 10.1038/s41396-021-01153-z. PubMed PMID: 34857933; PubMed Central PMCID: PMCPMC8941000.

51. Ortiz A, Vega NM, Ratzke C, Gore J. Interspecies bacterial competition regulates community assembly in the C. elegans intestine. ISME J. 2021;15(7):2131-45. Epub 20210215. doi: 10.1038/s41396-021-00910-4. PubMed PMID: 33589765; PubMed Central PMCID: PMCPMC8245486.

52. Carlstrom CI, Field CM, Bortfeld-Miller M, Muller B, Sunagawa S, Vorholt JA. Synthetic microbiota reveal priority effects and keystone strains in the Arabidopsis phyllosphere. Nat Ecol Evol. 2019;3(10):1445-54. Epub 20190926. doi: 10.1038/s41559-019-0994-z. PubMed PMID: 31558832; PubMed Central PMCID: PMCPMC6774761.

53. Venturelli OS, Carr AC, Fisher G, Hsu RH, Lau R, Bowen BP, et al. Deciphering microbial interactions in synthetic human gut microbiome communities. Mol Syst Biol. 2018;14(6):e8157. Epub 20180621. doi: 10.15252/msb.20178157. PubMed PMID: 29930200; PubMed Central PMCID: PMCPMC6011841.

54. Meehan CJ, Beiko RG. A phylogenomic view of ecological specialization in the Lachnospiraceae, a family of digestive tract-associated bacteria. Genome Biol Evol. 2014;6(3):703-13. doi: 10.1093/gbe/evu050. PubMed PMID: 24625961; PubMed Central PMCID: PMCPMC3971600.

55. Vacca M, Celano G, Calabrese FM, Portincasa P, Gobbetti M, De Angelis M. The Controversial Role of Human Gut Lachnospiraceae. Microorganisms. 2020;8(4). Epub 20200415. doi: 10.3390/microorganisms8040573. PubMed PMID: 32326636; PubMed Central PMCID: PMCPMC7232163.

56. Stackebrandt E. The Family Lachnospiraceae. The Prokaryotes. 2014.

57. Costello EK, Stagaman K, Dethlefsen L, Bohannan BJ, Relman DA. The application of ecological theory toward an understanding of the human microbiome. Science. 2012;336(6086):1255-62. Epub 2012/06/08. doi: science.1224203 [pii] 10.1126/science.1224203. PubMed PMID: 22674335.

58. Walter J, Ley R. The human gut microbiome: ecology and recent evolutionary changes. Annual Review of Microbiology. 2011;65:411-29. Epub 2011/06/21. doi: 10.1146/annurev-micro-090110-102830. PubMed PMID: 21682646.

59. McMurdie PJ, Holmes S. phyloseq: an R package for reproducible interactive analysis and graphics of microbiome census data. PLoS One. 2013;8(4):e61217. Epub 20130422. doi: 10.1371/journal.pone.0061217. PubMed PMID: 23630581; PubMed Central PMCID: PMCPMC3632530.

60. Yaqing Chen [aut c, Alvaro Gajardo [aut], Jianing Fan [aut], Zhong Q, Dubey P, Han K, et al. frechet: Statistical Analysis for Random Objects and Non-Euclidean Data. Available: https://CRANR-projectorg/package=frechet. 2020.

61. Schliep KP. phangorn: phylogenetic analysis in R. Bioinformatics. 2011;27(4):592-3. Epub 20101217. doi: 10.1093/bioinformatics/btq706. PubMed PMID: 21169378; PubMed Central PMCID: PMCPMC3035803.

62. Guillot G, Rousset F. Dismantling the Mantel tests. In: Harmon L, editor. Methods in Ecology and Evolution. 42013. p. 336–44.